SCIENTIFIC REPORTS

Two macrocycle-based sensors for anions sensing

Yingjie Liu[1], Zhixiang Zhao[2], Ran Huo[2] & Qingxiang Liu[2]

Two macrocyclic bis-benzimidazolium salts 2 and 4 (23-membered for 2 and 25-membered for 4) were prepared, and their structures were confirmed by X-ray crystallography, ^{1}H NMR and ^{13}C NMR spectroscopy. The research of anion recognitions using 2 or 4 as hosts were carried out with the methods of fluorescence and ultraviolet spectroscopy, ^{1}H NMR titrations, MS and IR spectra. The experiment results show that 2 can detect acetate anion and 4 can detect nitrate anion with favorable selectivity and sensitivity.

Anion recognition has attracted extensive attention in host-guest chemistry[1–3]. Among numerous anions, acetate group and nitrate group play very important roles in medical, biological and environmental areas. For example, sodium acetate can restrain the growth of microorganism and lengthen the shelf life of food[4–11]. Also, acetate group can participate in metabolic reactions in human body[12,13].

Nitrate salt as a pollutant exists extensively in the natural world, and it can be absorbed by crops from polluted water and soil. After these crops are consumed by human, the nitrate salt can be transformed into poisonous nitrite salt[14–18]. Hence, the detection of acetate group and nitrate group is of great importance for improving human health and protecting the environment. Some methods for detecting acetate group and nitrate group have been reported, such as fluorescence spectroscopy[19–22], ultraviolet spectroscopy[23–25] and ion chromatography[26,27]. By contrast, fluorescence method has been turned out to be simpler, more sensitive and easier to operate[28–30]. It is known that the change of fluorescence spectroscopy of host is mainly related to the interactions between host and guest. After the guest is added to the host, if fluorescence spectroscopy of host has remarkable change (such as enhancement, decrease or shift of emission peak), which shows that there exist strong interactions between the host and the guest. Otherwise, there are not obvious interactions between the host and the guest. The interaction forces between the host and the guest include mainly H-bonds, anion-π interactions and electrostatic interactions and so on[31–37], in which H-bonds are common interactions. To form H-bonds between the host and the guest, the introduction of some specific binding sites in the design of host is necessary (such as urea, thiourea, amide and imidazolium or benzimidazolium groups)[38–42].

In the process of seeking appropriate hosts, cyclic compounds with two benzimidazolium groups come into our sight. Because this type of hosts is good H-bond donors, they can combine with anionic guests through C-H···X hydrogen bonds[4,43,44]. In the paper, two new macrocyclic compounds with benzimidazolium moieties (2 and 4) are reported. The structures of 23-membered macrocycle 2 and 25-membered macrocycle 4 are confirmed by X-ray crystallography and ^{1}H NMR, ^{13}C NMR spectroscopy. The research of anion recognitions using 2 and 4 as hosts were carried out with the method of fluorescence spectroscopy, ^{1}H NMR titrations, HRMS and IR spectra.

Results and Discussion

Preparation and structures of macrocyclic compounds 2 and 4.
As shown in Fig. 1, the durene reacted with HBr and paraformaldehyde to give 1,4-di(bromomethyl)-durene, and then the reaction of 1,4-di(bromomethyl)-durene with KOH and benzimidazole afforded 1,4-di(benzimidazol-1-yl-methyl)-durene. 1,8-di(2′-bromoethoxy)-9,10-anthraquinone or 1,8-bis(3′-bromopropoxy)-9,10-anthraquinone were gotten through the reaction of 1,8-dihydroxy-9,10-anthraquinone with 1,2-dibromoethane or 1,3-dibromopropane, and they further reacted with 1,4-di(benzimidazol-1-yl-methyl)-durene to generate macrocyclic compounds 1 and 3 with two bromide anions. Compounds 2 or 4 (n = 2 for 2 and n = 3 for 4) were formed through the anion exchange reaction of compounds 1 or 3 with NH_4PF_6. Compounds 2 and 4 demonstrate excellent stability to air,

[1]Tianjin Key Laboratory of Process Measurement and Control, Institute of Robotics and Autonomous Systems, Tianjin University, Tianjin, 300072, China. [2]Key Laboratory of Inorganic-Organic Hybrid Functional Materials Chemistry (Tianjin Normal University), Ministry of Education; Tianjin Key Laboratory of Structure and Performance for Functional Molecules, College of Chemistry, Tianjin Normal University, Tianjin, 300387, China. Correspondence and requests for materials should be addressed to Q.L. (email: tjnulqx@163.com)
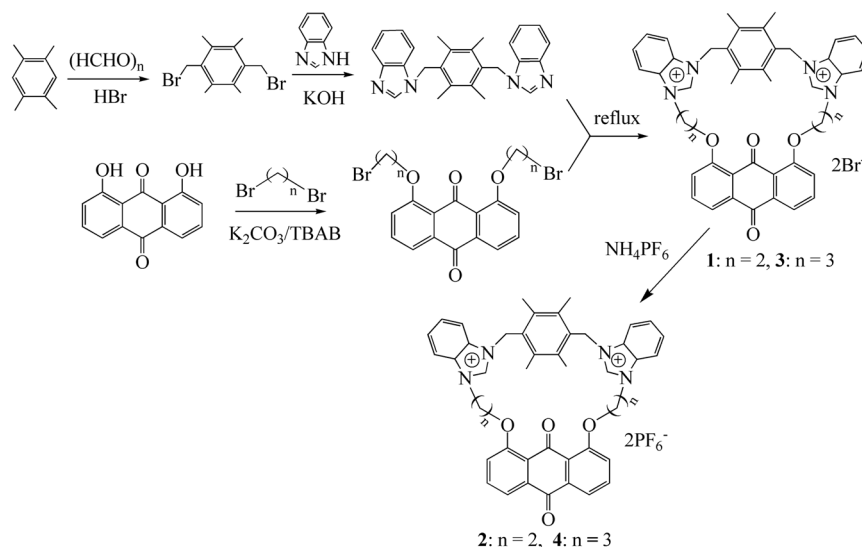
**Figure 1.** Preparation of macrocyclic compounds **2** and **4**.
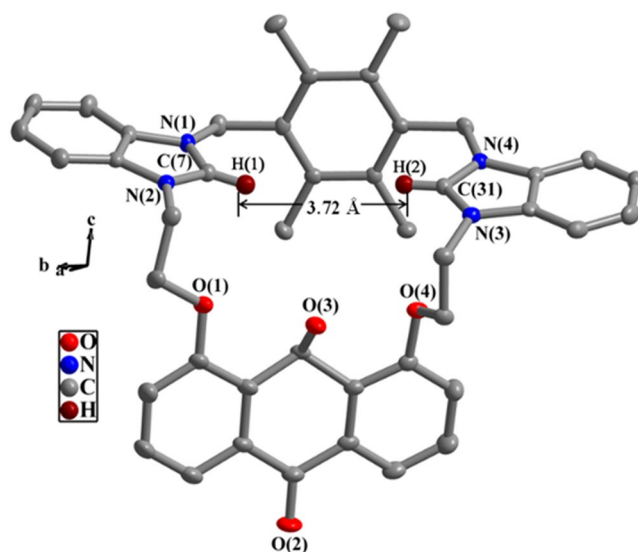
Figure 2. Crystal structure of compound **2**. Some bond lengths (Å) and angles (°): N(1)-C(7) 1.336(2), N(2)-C(7) 1.328(8), N(3)-C(31) 1.329(5), N(4)-C(31) 1.326(8); N(1)-C(7)-N(2) 110.3(2), N(3)-C(31)-N(4) 111.0(2).

moisture and heat, and their solubility are good in strong polar solvents like CH_3CN, CH_2Cl_2 and DMSO, but they are almost insoluble in nonpolar organinc solvents such as benzene and hexane. In the ^1H NMR spectra of **2** and **4**, the chemical shift of benzimidazolium proton signals (NC*H*N, $\delta = 8.82$ ppm and 8.41 ppm) accords with the chemical shifts of known azolium salts[45–52].

23-Membered and 25-membered macrocycles in the molecular structures of **2** and **4** are observed (Figs 2 and 3). Two benzimidazole rings in **2** are approximately parallel with the dihedral angle of 13.9(1)°, whereas the dihedral angles between two benzimidazole rings in **4** are 71.8(2)°. This displays that the distorted degree of two benzimidazoles in **4** is larger than that in **2**. The distances between H(1) and H(2) in **2** (3.72 Å) is larger than that (3.32 Å) in **4**.

Recognition of acetate anion using compound 2 as a sensor.
The recognition of anions ($H_2PO_4^-$, HSO_4^-, OAc^-, NO_3^-, I^-, Br^-, Cl^- and F^-) using **2** as a sensor was carried out with the methods of fluorescence and ultraviolet spectroscopy in H_2O/CH_3CN (v/v = 1/1) mixed solvent at 25 °C. The compound **2** displayed a wide emission band around 380–495 nm as shown in Fig. 4 ($\lambda_{ex} = 254$ nm, the slit widths were 5 nm and 3 nm for the excitation and emission). This emission band was attributed to that of anthraquinone. The fluorescence intensity barely changed after adding 20 equiv. of $H_2PO_4^-$, HSO_4^-, NO_3^-, I^-, Br^-, Cl^- and F^-, respectively, to the
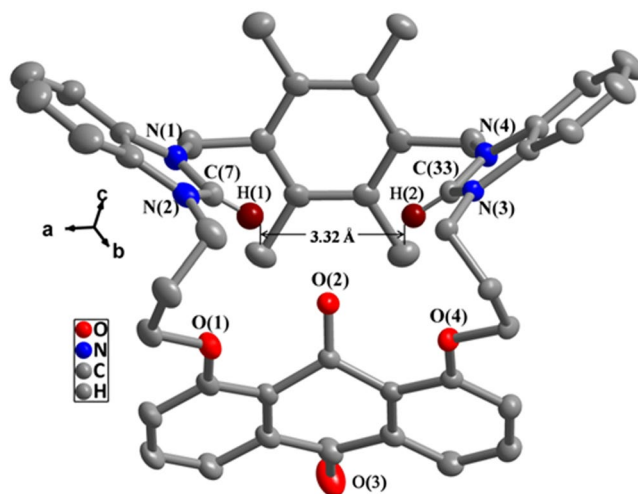
Figure 3. Crystal structure of compound **4**. All hydrogen atoms were omitted for clarity. Selected bond lengths (Å) and angles(°): N(1)-C(7) 1.330(5), N(2)-C(7) 1.324(5), N(3)-C(33) 1.320(4), N(4)-C(33) 1.323(4); N(1)-C(7)-N(2) 111.1(3), N(3)-C(33)-N(4) 111.2 (3).
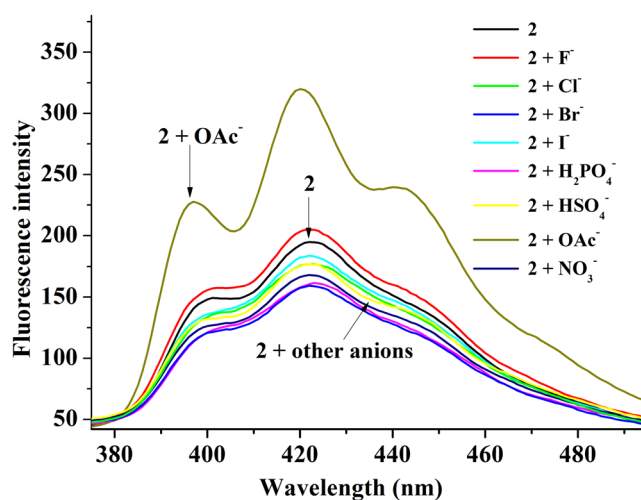

Figure 4. Fluorescence spectra of **2** (1×10^{-6} M) upon adding 20 equiv. of salts ($H_2PO_4^-$, HSO_4^-, OAc^-, NO_3^-, I^-, Br^-, Cl^- and F^-, and tetrabutyl ammonium being their cations) in H_2O/CH_3CN (v:v = 1:1) (λ_{ex} = 254 nm, slit: em = 3 nm, ex = 5 nm) at 25 °C.

solutions of **2**. However, adding 20 equiv. of OAc^- caused the remarkable enhancement of fluorescence intensity around 380–495 nm. In Fig. S1, the ultraviolet absorption of **2** at 230–280 nm increased distinctly with the addition of OAc^-. These experimental results demonstrated that **2** can discriminate effectively OAc^- from other anions. Thus, compound **2** may be functioned as a fluorescence chemosensor with high selectivity for OAc^-.

As shown in Fig. 5, the fluorescent titration experiments displayed that the fluorescence intensities of **2** around 380–495 nm enhanced gradually along with the incremental concentration of OAc^-. In the inset of Fig. 5, when the value of C_{OAc^-}/C_2 was between 0 to 44, the fluorescence intensities display rapid increases along with the incremental concentration of OAc^-. When the value exceeded 44:1, the enhancement of fluorescence intensities slowed down. When the value exceeded 54:1, more OAc^- would not cause further rise of fluorescent intensities. The increasing behavior of OAc^- about the fluorescence of **2** followed a Stern-Volmer equation (1)[53,54].

$$F_0/F = 1 + K_{SV}C_{OAc^-} \tag{1}$$

in which F and F_0 are the fluorescence intensities of **2** with and without OAc^-, and C_{OAc^-} is the concentration of OAc^-. The calculated constant K_{SV} for **2**·OAc^- is 1.2×10^4 M^{-1} (R = 0.996) through employing the equation (1), and the linear parts are in the ranges of $0–44 \times 10^{-6}$ M (Fig. S2). As shown in Fig. S3, the detection limit was determined to be 2.1×10^{-7} M according to the changes in OAc^- dependent fluorescence intensities[55].
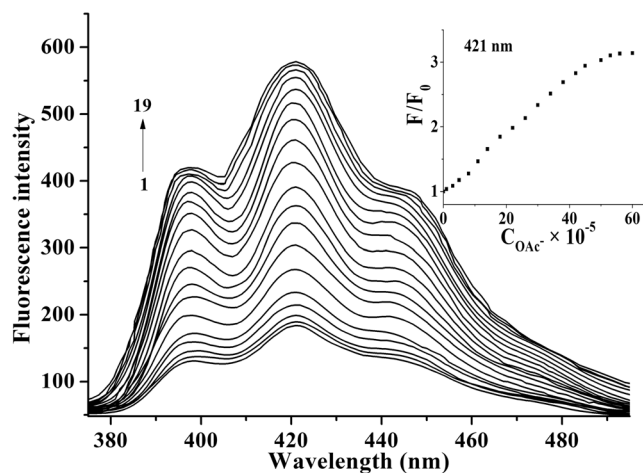
Figure 5. Fluorescent titration curves of **2** (1.0×10^{-6} M) in the existence of various concentrations of OAc⁻ in H₂O/CH₃CN (v/v = 1/1). C_{OAc^-} for curves 1–19 are 0, 0.2, 0.5, 1, 1.6, 2.4, 4, 8, 14, 20, 24, 28, 32, 36, 40, 44, 48, 54, 60×10^{-6} M ($\lambda_{ex} = 254$ nm). Inset: F/F_0 of **2** at 421 nm as a function of C_{OAc^-} ($\lambda_{ex} = 254$ nm, slit: em = 3 nm, ex = 5 nm) at 25 °C.
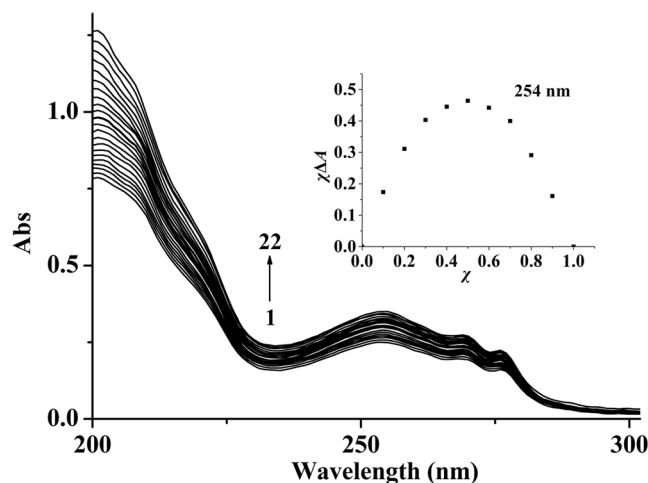
Figure 6. Ultraviolet absorption curves of **2** (1×10^{-5} M) in H₂O/CH₃CN (v:v = 1:1) at 25 °C. The concentrations of OAc⁻ for curves 1–22 are: 0, 0.4, 0.8, 1.2, 1.6, 3, 4, 6, 9, 12, 15, 18, 21, 24, 27, 30, 33, 38, 43, 48, 54, 60×10^{-5} M. Inset: the Job's plot for a **2**·OAc⁻ complex at 254 nm. χ is molar fractions of **2**, and $\chi\Delta A$ is the products between molar fractions and the discrepancy of the absorption bands.

In ultraviolet titration experiments (Fig. 6), the ultraviolet absorption of **2** enhanced gradually along with the increasing concentration of OAc⁻. The stability constant (K_S) was calculated according to the following relation of non-linear least square analysis of the titration curves for 1:1 complexation[56].

$$\Delta A = B\{C_2 + C_{OAc^-} + 1/K_S - [(C_2 + C_{OAc^-} + 1/K_S)^2 - 4C_2C_{OAc^-}]^{1/2}\} \tag{2}$$

where ΔA is the discrepancy between the absorbance with or without OAc⁻ ($\Delta A = A - A_0$), B is a floating parameter, C_{OAc^-} and C_2 are the concentrations of guest and host.

As displayed in Fig. S4, the plot of ΔA versus C_{OAc^-} showed good non-linear relationship for OAc⁻, which indicates the formation of 1:1 complexation between **2** and OAc⁻. The stability constant K_S was 2.3×10^4 M⁻¹ (R = 0.991). Noteworthy, Job's plot at 254 nm also further demonstrated to form a 1:1 complexation for **2**·OAc⁻ (Inset of Fig. 6)[57–59]. In the recognition of OAc⁻ using **2** as a host, the K_{SV} value (1.2×10^4 M⁻¹) from the fluorescence method and the K_S value (2.3×10^4 M⁻¹) from the ultraviolet method are consistent with each other[60]. Compared to the literatures, the binding constants of **2** to OAc⁻ are in the middle of the values of literatures reported, and the detection limit of **2** to OAc⁻ is close to the minimum in literatures reported (the binding constants and detection limits of these reports being in the range of 6.9×10^2 M⁻¹ to 5.9×10^5 M⁻¹ and 1.2×10^{-7} mol/L to 1.0×10^{-6} mol/L)[10,11,19–21,23,24,26].
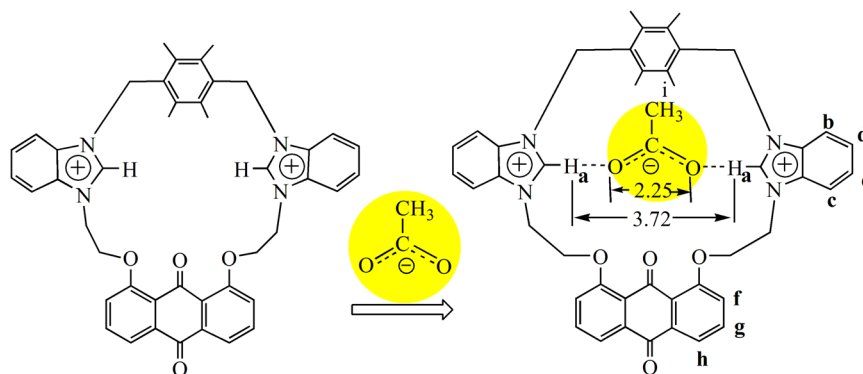
Figure 7. The interactions of OAc⁻ with **2**.
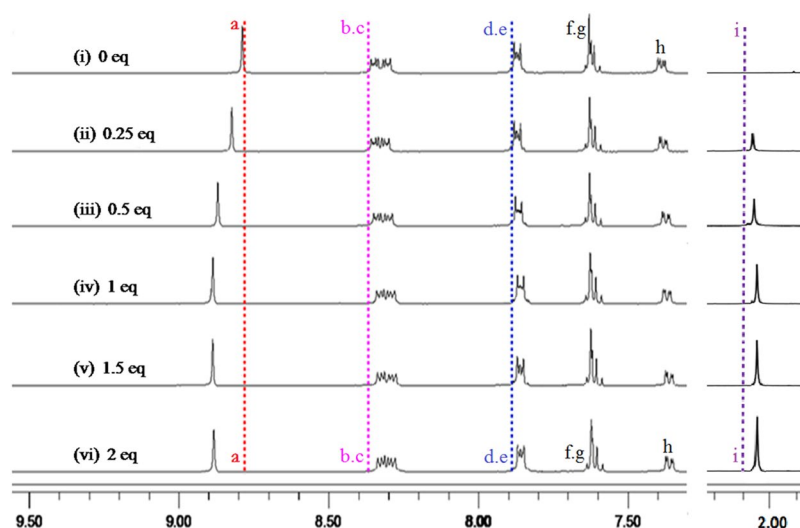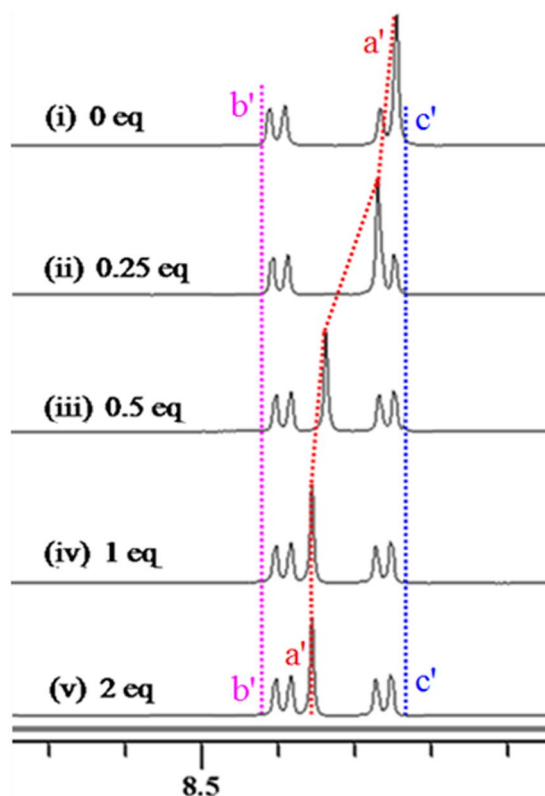

Figure 8. Partial ^{1}H NMR spectra. (i) **2**; (ii) **2** and 0.25 equivalent of OAc⁻; (iii) **2** and 0.5 equivalent of OAc⁻; (iv) **2** and 1 equivalent of OAc⁻; (v) **2** and 1.5 equivalent of OAc⁻; (vi) **2** and 2 equivalent of OAc⁻.

In competition experiments, 20 equiv. of other anions ($H_2PO_4^-$, HSO_4^-, NO_3^-, I^-, Br^-, Cl^- and F^-) was mixed with **2** (1×10^{-6} M), and then 20 equiv. of OAc⁻ was added. The fluorescence spectra show that there is no obvious enhancement or decrease in the existence of 20 equiv. of interfering anions (Fig. S5). The results show that **2** has the immunity from interference of other anions.

Interactions of acetate anion with 2. Through analyzing the cavity size and structure characteristics of **2** ($H(1)\cdots H(2)$ separation being 3.72 Å in Fig. 2), the size of OAc⁻ (the distance of two oxygen atoms in OAc⁻ being 2.25 Å)[61] is suitable with that of **2**. As shown in Fig. 7, Ha of host **2** is the most possible binding site for OAc⁻ and the acting force between **2** and OAc⁻ may be C-H···O hydrogen bonds. To gain related information about the binding mode of **2** and OAc⁻, ^{1}H NMR titration experiments was performed in DMSO-d_6 (Fig. 8). As displayed in Fig. 8(iv), the chemical shifts of Ha shifted downfield by 0.10 ppm, and the chemical shifts of Hb-He shifted upfield by 0.02–0.03 ppm in the presence of 1 equiv. of OAc⁻. Additionally, the chemical shifts of Hf decreased by 0.03 ppm. These results indicated there existed C-H···O hydrogen bonds between **2** and OAc⁻. By comparison of Fig. 8(v,vi), chemical shifts of protons (Ha-Hf) did not have further change in the presence of more OAc⁻, which proved the formation of 1:1 complexation between **2** and OAc⁻. In HRMS of **2**·OAc⁻ (Fig. S14), m/z (747.29) of $[\mathbf{2} - 2(PF_6^-) + OAc^-]^+$ was observed, which further confirmed that a 1:1 complexation between **2** and OAc⁻ was formed. All these results accorded with the survey of the Job's plot experiment (Fig. 5). To further know the complexation property of **2** with OAc⁻, IR spectra of free **2**, OAc⁻ and **2**·OAc⁻ were measured (Fig. S16). The C-H flexural vibration bands moved from 841 cm⁻¹ in free **2** to 837 cm⁻¹ in **2**·OAc⁻, and the C-H stretching vibration moved from 2959 cm⁻¹ in free OAc⁻ to 2962 cm⁻¹ in **2**·OAc⁻. The C=O bands of OAc⁻ moved from 1677 cm⁻¹ in OAc⁻ to 1667 cm⁻¹ in **2**·OAc⁻. The C-N bands moved from 1587 cm⁻¹ in free **2** to 1584 cm⁻¹ in **2**·OAc⁻.

Through the comprehensive analysis of ^{1}H NMR titrations, HRMS spectra, IR spectra and structure of **2**, the binding force between **2** and OAc⁻ is mainly attributed to C-H···O hydrogen bonds because of strong affinity of hydrogen atom toward oxygen atom. Upon the combination of **2** and OAc⁻, the fluorescence intensity of **2**

Figure 9. Partial ^{1}H NMR spectra in DMSO-d_6. (i) **4**; (ii) **4** and 0.25 equivalent of NO_3^-; (iii) **4** and 0.5 equivalent of NO_3^-; (iv) **4** and 1 equivalent of NO_3^-; (v) **4** and 2 equivalent of NO_3^-.

enhanced remarkably. We tried to the cultivation of single crystal for **2**·OAc$^-$ to determine its solid-state structure. Unfortunately, no single crystals can be gotten.

Recognition of nitrate anion using 4 as a sensor.

The selective recognition of some anions ($H_2PO_4^-$, HSO_4^-, OAc$^-$, NO_3^-, I$^-$, Br$^-$, Cl$^-$ and F$^-$, and their cations being tetrabutyl ammonium (TBA$^+$)) using **4** as a sensor was also investigated by using analogous methods of **2** for OAc$^-$. The results showed that **4** was a highly selective fluorescent sensor for NO_3^-, and it can discriminate between NO_3^- and other anions (Figs S6–S13). The Stern-Volmer constant K_{SV} value was calculated as $1.5 \times 10^4 \, M^{-1}$ (R = 0.998) for **4**·NO_3^- based on fluorescence method (Fig. S9), and it was similar to the stability constant K_S value ($2.5 \times 10^4 \, M^{-1}$) from the UV/vis method (Fig. S12)[60]. The detection limit (2.6×10^{-7} M) was estimated from the changes in NO_3^- dependent fluorescence intensity (Fig. S10), and this value is in the middle of the values of the literatures (the detection limits of these reports are in the range of 4.7×10^{-7}–1.7×10^{-8} mol/L)[22,25,27].

The spectral differences in ^{1}H NMR titration experiments of **4** are depicted in Fig. 9. *H*a' has a large shift (0.12 ppm) with the addition of 1 equiv. of NO_3^- as shown in Fig. 9(iv). At the same time, the signals of *H*b' and *H*c' shifted upfield by 0.02 ppm upon addition of 1 equiv. of NO_3^-. These changes should be attributed to the formation of C-H···O hydrogen bonds between NO_3^- and C(2)-H of benzimidazolium (Fig. 10). In addition, the chemical shifts of the other protons in **4** do not obviously change upon the addition of more equivalents of NO_3^- (Fig. 9(v)). This indicates that a 1:1 complex between **4** and NO_3^- was formed. In high resolution mass spectrometry (HRMS) analysis of **4**·NO_3^- (Fig. S15), m/z (778.30) of $[4 - 2(PF_6^-) + NO_3^-]^+$ is observed, which provides additional evidence for the formation of a 1:1 complex between **4** and NO_3^-. These results are consistent with the result of the Job's plot experiment (Inset of Fig. S11).

To further understand the complexation behavior of **4** with NO_3^-, the infrared spectra (IR) of **4**, NO_3^- and **4**·NO_3^- were measured. In the infrared spectra (Fig. S17), we observed that N=O absorption bands of NO_3^- move from 1338 cm^{-1} in NO_3^- to 1347 cm^{-1} in **4**·NO_3^-, C-H flexural vibration absorption bands move from 747 cm^{-1} in free **4** to 751 cm^{-1} in **4**·NO_3^-, and the C-H stretching vibration in free **4** move from 2954 cm^{-1} in free **4** to 2963 cm^{-1} in **4**·NO_3^-. The C-N flexural vibration absorption bands move from 1583 cm^{-1} in free **4** to 1589 cm^{-1} in **4**·NO_3^-.

Applications of 2 or 4 in real samples.

The practical applications of **2** or **4** were estimated through the determination of OAc$^-$ or NO_3^- added in real water samples (tap water and drinking water). The water samples were mixed with known concentrations of OAc$^-$ (8.0×10^{-6} mol/L) or NO_3^- (15.0×10^{-6} mol/L) and analyzed by the standard methods. Each sample was analyzed with their three replicates. The results were summarized in
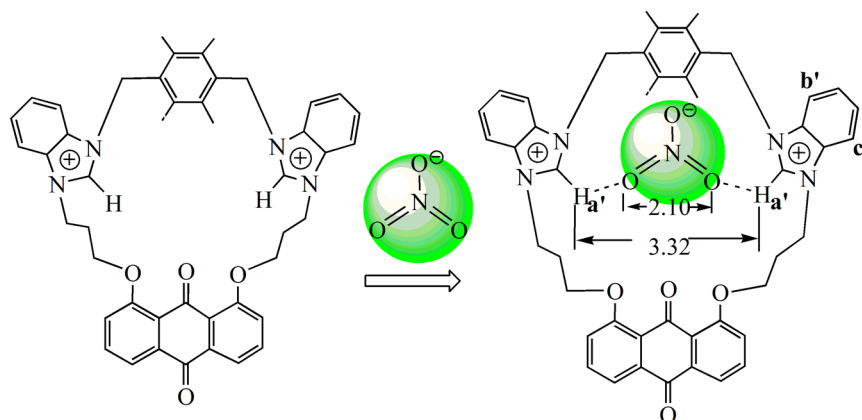
Figure 10. The interactions of NO_3^- with **4**.

Sample	OAc⁻ added (μM)	OAc⁻ found (μM)	RSD[a] (%)
Tap water	8.00	8.20	2.57
Drinking water	8.00	7.80	1.61

Table 1. Application of **2** in real samples. [a]Relative standard deviation of three individual measurements.

Sample	NO₃⁻ added (μM)	NO₃⁻ found (μM)	RSD[a] (%)
Tap water	15.00	15.10	2.05
Drinking water	15.00	14.70	1.86

Table 2. Application of **4** in real samples. [a]Relative standard deviation of three individual measurements.

Tables 1 and 2, and these results had small relative standard deviation (RSD) values. Therefore, the sensors **2** or **4** have potential application ability for OAc⁻ or NO₃⁻ in real samples.

Conclusion

In summary, two new 23-membered and 25-membered macrocyclic compounds **2** and **4** with bis-benzimidazolium groups have been synthesized and characterized. The anion recognition abilities of **2** or **4** have been investigated. The fluorescence and ultraviolet titrations show that **2** can detect effectively acetate anion. The K_{SV} value ($1.2 \times 10^4\,M^{-1}$) and K_S value ($2.3 \times 10^4\,M^{-1}$) for **2**·OAc⁻ are similar to each other. Even if the detection limit is down to $2.1 \times 10^{-7}\,mol/L$, the detection of **2** to OAc⁻ is sensitive. Analogously, **4** has special selectivity for nitrate anion. The K_{SV} value ($1.5 \times 10^4\,M^{-1}$) and K_S value ($2.5 \times 10^4\,M^{-1}$) for **4**·NO₃⁻ are too similar to each other. Even if the detection limit is down to $2.6 \times 10^{-7}\,mol/L$, the detection of **4** to NO₃⁻ is sensitive. The differences between **2** and **4** in the course of anion recognitions are mainly related to the structural characteristics of the macrocycles. The distance between two C(2)-H of benzimidazolium in **2** (3.72 Å) is larger than that in **4** (3.32 Å), therefore, **2** can effectively match with OAc⁻, and **4** can match effectively with NO₃⁻ (the distance between two oxygen atoms in OAc⁻ (2.25 Å) being larger than in NO₃⁻ (2.10 Å)). The experiment results reveal that compounds **2** and **4** have good application prospects in anion recognitions. Our ongoing research is aiming at recognizing anions more efficiently, and the development of some environment-friendly, highly selective and highly sensitive chemosensors are underway.

Experimental

General procedures. Total commercially available chemicals for synthesis and test were of reagent grade. A Boetius Block apparatus was used for the report of melting points. A PerkinElmer Spectrum 100 FT-IR spectrophotometer was used for the report of Infrared (IR) spectra. A Varian spectrometers was used for the report of ¹H NMR and ¹³C NMR spectra. The measurement of the elemental analyses was carried out on a Perkin-Elmer 2400C Elemental Analyzer. Ultraviolet spectra were recorded on a PerkinElmer Lamber35 UV spectrophotometer. The fluorescence spectra were carried out in a Shimadzu RF-5301PC fluorescence spectrophotometer. A VG ZAB-HS mass spectrometer was used to record EI mass spectra.

1,4-Di(benzimidazole-methyl)-durene. 10 mL of HBr/acetic acid solution (31 wt%) was added to the glacial acetic acid (30 mL) solution of durene (6.710 g, 50.0 mmol) and paraformaldehyde (3.075 g, 102.5 mmol). The mixture was heated at 120 °C for 8 hours, and then this mixture was poured into 50 mL of H₂O to precipitate a

white powder, which was collected through filtration to give 1,4-di(bromomethyl)-durene. Yield: 15.205 g (95%). M.p.: 192–194 °C.

TBAB (0.260 g, 0.8 mmol), KOH (2.000 g, 35.6 mmol) and benzimidazole (2.150 g, 18.2 mmol) were added to 100 mL of CH$_3$CN, and this suspension was stirred under refluxing for 1 hour. To above mixture was drop-wise added a CH$_3$CN (50 mL) solution of 1,4-di(bromomethyl)-durene (2.880 g, 9.0 mmol), and the reaction was carried out at 80 °C for 72 hours. After CH$_3$CN was removed via rotary evaporation, CH$_2$Cl$_2$ (100 mL) was added to the residue, which was washed with water (3 × 100 mL). The CH$_2$Cl$_2$ solution was dried over anhydrous MgSO$_4$. After CH$_2$Cl$_2$ was removed via rotary evaporation, a white powder of 1,4-di(benzimidazol-1-yl-methyl)-durene was gotten. Yield: 3.014 g (86%). Anal. Calcd for C$_{26}$H$_{26}$N$_4$: C, 79.14; H, 6.65; N, 14.21%. Found: C, 79.32; H, 6.79; N, 14.42%. M.p.: 238–240 °C. ^{1}H NMR (400 MHz, DMSO-d_6): δ 2.21 (s, 12H, CH$_3$), 5.51 (s, 4H, CH$_2$), 7.31 (m, 4H, ArH), 7.63 (d, J = 7.6 Hz, 2H, PhH), 7.68 (d, J = 7.6 Hz, 2H, ArH), 7.72 (s, 2H, 2-benzimH) (benzim = benzimidazole).

1,8-Di(2′-bromoethoxy)-9,10-anthraquinone. 1,2-Dibromoethane (4.691 g, 24.9 mmol) was drop-wise added to a suspension of anhydrous K$_2$CO$_3$ (3.446 g, 24.8 mmol), 1,8-dihydroxy-9,10-anthraquinone (1.082 1.000 g, 4.1 mmol), TBAB (0.184 g, 0.5 mmol) in acetone (50 mL), and the mixture was stirred under refluxing for 72 hours. After acetone was removed, 60 mL of water was added to the residue. The aqueous was extracted with CH$_2$Cl$_2$ (3 × 30 mL) and the combined solvent was removed via rotary evaporation after drying over anhydrous MgSO$_4$. A yellow powder of 1,8-di(2′-bromoethoxy)-9,10-anthraquinone was gotten. Yield: 1.133 g (60%). Anal. Calcd for C$_{18}$H$_{14}$Br$_2$O$_4$: C, 47.61; H, 3.11%. Found: C, 47.84; H, 3.44%. M.p.: 122–124 °C. ^{1}H NMR (400 MHz, DMSO-d_6): δ 3.86 (t, J = 5.8 Hz, 4H, CH$_2$), 4.50 (t, J = 5.8 Hz, 4H, CH$_2$), 7.58 (q, J = 3.2 Hz, 2H, ArH), 7.76 (t, J = 2.8 Hz, 4H, ArH). ^{13}C NMR (100 MHz, DMSO-d_6): δ 182.8 (C=O), 180.7 (C=O), 157.3 (ArC), 134.2 (ArC), 134.1 (ArC), 124.2 (ArC), 121.5 (ArC), 119.2 (ArC), 69.7 (OCH$_2$CH$_2$), 30.8 (OCH$_2$CH$_2$).

1,8-Bis(3′-bromopropoxy)-9,10-anthraquinone. This compound was prepared in a manner analogous to that for 1,8-bis(2′-bromoethoxy)-9,10-anthraquinone, only 1,3-dibromopropane (5.450 g, 27.0 mmol) was used instead of 1,2-dibromoethane. Yield: 1.735 g (80%). M.p.: 145–147 °C. Anal. Calcd for C$_{20}$H$_{18}$Br$_2$O$_4$: C, 49.82; H, 3.76%. Found: C, 49.83; H, 3.84%. ^{1}H NMR (400 MH$_Z$, DMSO-d_6): δ 2.10 (m, 4H, CH$_2$), 3.65 (t, J = 6.6 Hz, 4H, CH$_2$), 4.01 (t, J = 5.6 Hz, 4H, CH$_2$), 7.33 (t, J = 4.2 Hz, 2H, ArH), 7.53 (m, 4H, ArH). ^{13}C NMR (100 MH$_Z$, DMSO-d_6): δ 183.5 (C=O), 181.9 (C=O), 157.5 (ArC), 141.8 (ArC), 135.4 (ArC), 134.3 (ArC), 132.4 (ArC), 131.6 (ArC), 130.9 (ArC), 127.5 (ArC), 127.4 (ArC), 123.8 (ArC), 114.40 (ArC), 45.2 (CH$_2$), 31.2 (CH$_2$), 16.3 (CH$_2$).

Macrocyclic Compound 2. To a CH$_3$CN (200 mL) solution of 1,8-di(2′-bromoethoxy)-9,10-anthraquinone (0.455 g, 1.0 mmol) was added a CH$_3$CN (200 mL) solution of 1,4-di(benzimidazol-1-yl-methyl)-durene (0.394 g, 1.0 mmol). After refluxing for 48 hours, a yellow solid was generated. The solid was collected through filtration to afford macrocyclic compound **1** with two bromide anions.

A solution of NH$_4$PF$_6$ (0.391 g, 2.3 mmol) in methanol (20 mL) was added to a solution of compound **1** (0.878 g, 1.0 mmol) in methanol (40 mL), and then the mixed solution was stirred for 2.5 days at 25 °C to precipitate a pale yellow solid. The solid was collected through filtration to give macrocyclic compound **2** with two hexafluorophosphate anions. M.p.: 282–284 °C. Yield: 0.723 g (74%). Anal. Calcd for C$_{44}$H$_{40}$F$_{12}$N$_4$O$_4$P$_2$: C, 53.99; H, 4.11; N, 5.72%. Found: C, 53.87; H, 4.23; N, 5.65%. ^{1}H NMR (400 MHz, DMSO-d_6): δ 2.05 (s, 12H, CH$_3$), 4.51 (d, J = 3.6 Hz, 4H, OCH$_2$CH$_2$), 5.05 (d, J = 4.0 Hz, 4H, OCH$_2$CH$_2$), 5.78 (s, 4H, CH$_2$), 7.40 (q, J = 3.2 Hz, 2H, ArH), 7.62 (t, J = 3.2 Hz, 4H, ArH), 7.87 (q, J = 3.2 Hz, 4H, ArH), 8.36 (m, 4H, ArH), 8.82 (s, 2H, 2-benzimH). ^{13}C NMR (100 MHz, DMSO-d_6): δ 183.4 (C=O), 182.2 (C=O), 156.1 (ArC), 142.6 (ArC), 134.9 (ArC), 134.5 (ArC), 131.1 (ArC), 126.2 (ArC), 121.7 (ArC), 120.3 (ArC), 119.0 (ArC), 113.5 (ArC), 67.8 (OCH$_2$CH$_2$), 44.7 (NCH$_2$), 30.6 (NCH$_2$), 16.3 (CH$_3$), 15.8 (CH$_3$).

Macrocyclic Compound 4. This compound was prepared in a manner analogous to that for compound **2**, only 1,8-bis(3'-bromopropoxy)-9,10-anthraquinone (0.482 g, 1.0 mmol) was used instead of 1,8-bis(2′-bromoethoxy)-9,10-anthraquinone. Yield: 0.795 g (79%). M.p.: 286–288 °C. Anal. Calcd for C$_{46}$H$_{44}$F$_{12}$N$_4$O$_4$P$_2$: C, 54.87; H, 4.40; N, 5.56%. Found: C, 54.74; H, 4.52; N, 5.63%. ^{1}H NMR (400 MHz, DMSO-d_6): δ 1.85 (s, 12H, CH$_3$), 2.49 (d, J = 1.6 Hz, 4H, OCH$_2$CH$_2$CH$_2$), 3.93 (t, J = 5.4 Hz, 4H, OCH$_2$CH$_2$CH$_2$), 4.80 (t, J = 6.4 Hz, 4H, OCH$_2$CH$_2$CH$_2$), 5.71 (s, 4H, CH$_2$), 7.40 (q, J = 3.2 Hz, 2H, ArH), 7.85 (m, 8H, ArH), 8.26 (d, J = 8.4 Hz, 4H, ArH), 8.41 (d, J = 8.0 Hz, 2H, 2-benzimH). ^{13}C NMR (100 MHz, DMSO-d_6): δ 183.5 (C=O), 182.4 (C=O), 157.5 (PhC), 141.8 (ArC), 135.4 (ArC), 134.3 (ArC), 132.4 (ArC), 131.6 (ArC), 130.9 (ArC), 127.5 (ArC), 123.8 (ArC), 120.7 (ArC), 119.3 (ArC), 114.4 (ArC), 69.0 (OCH$_2$CH$_2$), 53.2 (NCH$_2$), 45.1 (NCH$_2$), 31.1 (CH$_3$CH$_2$CH$_3$), 26.1 (CH$_3$), 16.2 (CH$_3$).

Fluorescence Titrations. The stock solution (1.0×10^{-4} M) of the host was prepared and diluted to the suitable concentration with H$_2$O/CH$_3$CN (v:v = 1:1). The stock solutions (1.0×10^{-4} M or 1.0×10^{-3} M) of guest were prepared and diluted in the same solvent. Test solutions were prepared through placing 0.1 mL of host stock solution into a 10 mL volumetric flask, and the appropriate amount of the stock solutions (1.0×10^{-4} M or 1.0×10^{-3} M) of guest were added with a microsyringe. The mixture solutions were diluted to 10 mL with H$_2$O/CH$_3$CN (1:1) to prepare test solutions. The concentrations of guest in the test solutions were from 0 to 60.0×10^{-6} M, and the concentration of host stayed the same (1.0×10^{-6} M). The test solutions were kept at 25 °C for 10 minutes, and then fluorescence spectra were recorded with the excitation wavelength at 254 nm. Stern-Volmer constant K_{SV} was derived from plots of F_0/F vs C_{OAc}− $\times 10^{-6}$ (or C_{NO3}− $\times 10^{-6}$) using Origin 8.0.

Job's plot. The stock solution (1.0×10^{-4} M) of the host was prepared and diluted to the suitable concentration with H$_2$O/CH$_3$CN (v:v = 1:1). The stock solutions (1.0×10^{-4} M or 1.0×10^{-3} M) of tetrabutylammonium

salts of $H_2PO_4^-$, HSO_4^-, OAc^-, NO_3^-, I^-, Br^-, Cl^- and F^- were prepared and diluted in the same solvent. Test solutions were prepared through placing 1 mL of host stock solution into a volumetric flask of 10 mL, and the appropriate amount of the stock solutions (1.0×10^{-4} M or 1.0×10^{-3} M) of tetrabutylammonium salts were added with a microsyringe. The mixture solutions were diluted to 10 mL with H_2O/CH_3CN (1:1) to prepare test solutions. The molar fractions of host and anion in the test solutions were from 1 to 0 and 0 to 1, respectively. The total concentration is 1.0×10^{-5} M. The test solutions were kept at 25 °C for 10 minutes, and then absoption spectra were measured.

Ultraviolet titrations. According to the methods in fluorescence titrations, the stock solutions and test solutions of UV/vis titrations were prepared. The concentrations of guest in the test solutions were from 0 to 60.0×10^{-5} M, and the concentration of host stayed the same (1.0×10^{-5} M). The test solutions were kept at 25 °C for 10 minutes, and then absoption spectra were measured.

Real sample analysis. The stock solution (1.0×10^{-4} M) of the host was prepared and diluted to the suitable concentration with H_2O/CH_3CN (v:v = 1:1). The stock solutions (1.0×10^{-4} M or 1.0×10^{-3} M) of guest were prepared and diluted in the same solvent. The tap water and drinking water were obtained from the college of chemistry, Tianjin Normal University. Different anions were added in the real water samples. Test solutions were prepared according to the methods in fluorescence titrations. The concentrations of OAc^- or NO_3^- were 8.0×10^{-6} M and 15.0×10^{-6} M, respectively. The test solutions were kept at 25 °C for 10 minutes, and then fluorescence spectra were recorded with the excitation wavelength at 254 nm.

X-ray structure determinations. A Bruker Apex II CCD diffractometer were used for the collection of diffraction data of **2** and **4**[62]. The structure was solved with the SHELXS program[63]. Figures 1 and 2 were formed via employing Crystal-Maker[64]. Other details for structural analysis and crystallographic data was listed in Table S1.

References

1. Yao, H. *et al.* A novel supramolecular AIE gel acts as a multi-analyte sensor array. *New J. Chem.* **42**, 18059–18065 (2018).
2. Santos-Figueroa, L. E. *et al.* Chromogenic and fluorogenic chemosensors and reagents for anions. A comprehensive review of the years 2010–2011. *Chem. Soc. Rev.* **42**, 3489–3613 (2013).
3. Shumilova, T. A., Rüffer, T., Lang, H. & Kataev, E. A. Straightforward design of fluorescent receptors for sulfate: Study of non-covalent interactions contributing to host-guest formation. *Chem. Eur. J.* **24**, 1500–1504 (2018).
4. Lu, Q. S. *et al.* Imidazolium-functionalized BINOL as a multifunctional receptor for chromogenic and chiral anion recognition. *Org. Lett.* **11**, 669–672 (2009).
5. Akcil, A. Destruction of cyanide in gold mill effluents: Biological versus chemical treatments. *Biotech. Adv.* **21**, 501–511 (2003).
6. Pearce, L. L., Bominaar, E. L., Hill, B. C. & Peterson, J. Reversal of cyanide inhibition of cytochrome *c* oxidase by the auxiliary substrate nitric oxide. *J. Biol. Chem.* **278**, 52139–52145 (2003).
7. Cummings, T. F. The treatment of cyanide poisoning. *Occ. Med.* **54**, 82–85 (2004).
8. Manez, R. M. & Sancenon, F. Fluorogenic and chromogenic chemosensors and reagents for anions. *Chem. Rev.* **103**, 4419–4476 (2003).
9. Nishiyabu, R. & Anzenbacher, P. 1,3-Indane-based chromogenic calixpyrroles with push-pull chromophores: Synthesis and anion sensing. *Org. Lett.* **8**, 359–362 (2006).
10. Xu, K. *et al.* Novel anthracene-based fluorescent sensor for selective recognition of acetate anions in protic media. *Spectrochimi Acta A* **137**, 957–961 (2015).
11. Singh, A., Tom, S. & Trivedi, D. R. Aminophenol based colorimetric chemosensor for naked-eye detection of biologically important fluoride and acetate ions in organo-aqueous medium: Effective and simple anion sensors. *J. Photoch. Photobio. A* **353**, 507–520 (2018).
12. Manju, S., Jose, L., Gopal, T. K. S., Ravishankar, C. N. & Lalitha, K. V. Effects of sodium acetate dip treatment and vacuum-packaging on chemical, microbiological, textural and sensory changes of pearlspot (Etroplus suratensis) during chill storage. *Food Chem.* **102**, 699–706 (2007).
13. Sallam, K. I. Antimicrobial and antioxidant effects of sodium acetate, sodium lactate, and sodium citrate in refrigerated sliced salmon. *Food control* **18**, 566–575 (2007).
14. Bruning-Fann, C. S. & Kaneene, J. B. The effects of nitrate, nitrite and N-nitroso compounds on human health: a review. *Vet. Hum. Toxicol.* **35**, 521–538 (1993).
15. Knobeloch, L., Salna, B., Hogan, A., Postle, J. & Anderson, H. Blue babies and nitrate-contaminated well water. *Environ. Health Perspect.* **108**, 675–678 (2000).
16. Ke, G. H., Wang, P. & Yang, Z. Plant uptake of non-ionic organic chemicals. *Environ. Sci. Technol.* **29**, 45–47 (2006).
17. Butler, A. Nitrites and nitrates in the human diet: Carcinogens or beneficial hypotensive agents. *J. Ethnopharmacology* **167**, 105–107 (2015).
18. Chetty, A. A. & Prasad, S. Flow injection analysis of nitrate-N determination in root vegetables: Study of the effects of cooking. *Food Chem.* **116**, 561–566 (2009).
19. Pandian, T. S., Srinivasadesikan, V., Lin, M. C. & Kang, J. A. selective acetate anion binding receptor: Participation via cationic CH_3 donors. *Tetrahedron* **71**, 8350–8356 (2015).
20. Guadalupe Hernandez, J., Huerta-Aguilar, C. A., Thangarasu, P. & Hopfl, H. A ruthenium(III) complex derived from N,N′-bis(salicylidene)ethylenediamine as a chemosensor for the selective recognition of acetate and its interaction with cells for bioimaging: Experimental and theoretical studies. *New J. Chem.* **41**, 10815–10827 (2017).
21. Huang, W. W., Li, Y. P., Lin, H. & Lin, H. Colorimetric recognition of acetate anions in aqueous solution using charge neutral azo derivatives. *Spectrochimi. Acta A* **86**, 437–442 (2012).
22. Chen, S. Y. & Ni, X. L. Development of an AIE based fluorescent probe for the detection of nitrate anions in aqueous solution over a wide pH range. *RSC Adv.* **6**, 6997–7001 (2016).
23. Singh, A. & Trivedi, D. R. 'Naked-eye' detection of biologically important anions in aqueous media by colorimetric receptor and its real life applications. *Spectrochimi Acta A* **179**, 95–103 (2017).
24. Sekutor, M., Opacak, S., Aleskovic, M. & Mlinaric-Majerski, K. Synthesis and anion binding properties of a novel 1,8-dipyrrolecarbazole Schiff base. *Croat. Chem. Acta* **88**, 405–411 (2015).
25. Tan, J. Y. *et al.* Chalcone based ion-pair recognition towards nitrates and the application for the colorimetric and fluorescence turn-on determination of water content in organic solvents. *Sensor. Actuat. B-Chem.* **260**, 727–735 (2018).
26. Qasem, R. J., Farh, I. K. & Essa, M. A novel LC-MS/MS method for the quantitative measurement of the acetate content in pharmaceutical peptides. *J. Pharmaceut. Bio. Anal.* **146**, 354–360 (2017).

27. Nemade, K., Fegade, U., Attarde, S. & Ingle, S. Determination of nitrite and nitrate in water and leafy vegetable samples using ion chromatography with conductivity detection. *Chem. Sci. Rev. Lett.* **4**, 703–710 (2015).

28. Hu, Y. M., Wang, X. M., Fei, D., Dong, F. Q. & Ding, L. S. Study on the interaction between Riboflavin and herring sperm DNA by fluorescence spectrometry. *Acta Chim. Sinica* **66**, 1245–1251 (2008).

29. Wang, C. C. *et al.* A ratiometric fluorescent chemosensor for Hg^{2+} based on FRET and its application in living cells. *Sensor. Actuat. B-Chem.* **198**, 33–40 (2014).

30. Morteza, H. *et al.* Selective recognition of acetate ion based on fluorescence enhancement chemosensor. *Luminescence* **27**, 341–345 (2012).

31. Choi, K. & Hamilton, A. D. Selective anion binding by a macrocycle with convergent hydrogen bonding functionality. *J. Am. Chem. Soc.* **123**, 2456–2457 (2001).

32. Caballero, A. *et al.* Discovery of anion-π interactions in the recognition mechanism of inorganic anions by 1,2,3-triazolium rings. *Chem. Commun.* **50**, 4680–4682 (2014).

33. Guha, S. & Saha, S. Fluoride ion sensing by an anion-π interaction. *J. Am. Chem. Soc.* **132**, 17674–17677 (2010).

34. Barryman, O. B., Sather, A. C., Hay, B. P., Meisner, J. S. & Johnson, D. W. Solution phase measurement of both weak σ and C-H···X⁻ hydrogen bonding interactions in synthetic anion receptors. *J. Am. Chem. Soc.* **130**, 10895–10897 (2008).

35. Chifotides, H. T., Schottel, B. L. & Dunbar, K. R. The π-accepting arene HAT(CN)₆ as a halide receptor through charge transfer: Multisite anion interactions and self-assembly in solution and the solid state. *Angew. Chem., Int. Ed.* **49**, 7202–7207 (2010).

36. Rosokha, Y. S., Lindeman, S. V., Rosokha, S. V. & Kochi, J. K. Halide recognition through diagnostic "anion-π" interactions: Molecular complexes of Cl⁻, Br⁻, and I⁻ with olefinic and aromatic π receptors. *Angew. Chem., Int. Ed.* **43**, 4650–4652 (2004).

37. Gale, P. A., Howe, E. N. W. & Wu, X. Anion receptor chemistry. *Chem.* **1**, 351–422 (2016).

38. García-Garrido, S. E., Caltagirone, C., Light, M. E. & Gale, P. A. Acridinone-based anion receptors and sensors. *Chem. Commun.* **14**, 1450–1452 (2007).

39. Lorenzo, A., Aller, E. & Molina, P. Iminophosphorane-based synthesis of multinuclear ferrocenyl urea, thiourea and guanidine derivatives and exploration of their anion sensing properties. *Tetrahedron* **65**, 1397–1401 (2009).

40. Choi, J. K. *et al.* A PCT-based, pyrene-armed calix[4]crown fluoroionophore. *J. Org. Chem.* **71**, 8011–8015 (2006).

41. Hironori, I. *et al.* Novel 1,8-naphthalimide derivative with an open space for an anion: Unique fluorescence behaviour depending on the anion's electrophilic. *Chem. Commun.* **51**, 8596–8599 (2015).

42. Zhang, D. W. *et al.* Acridine-based macrocyclic fluorescent sensors: Self-assembly behavior characterized by crystal structures and a tunable bathochromic-shift in emission induced by H₂PO₄⁻ via adjusting the ring size and rigidity. *Org. Biomol. Chem.* **11**, 3375–3381 (2013).

43. Bakê, M. V. *et al.* Azolium-linked cyclophanes: A comprehensive examination of conformations by ¹H NMR spectroscopy and structural studies. *J. Org. Chem.* **69**, 7640–7652 (2004).

44. Kim, S. K. *et al.* New fluorescent photoinduced electron transfer chemosensor for the recognition of H₂PO₄⁻. *Org. Lett.* **5**, 2083–2086 (2003).

45. Hahn, F. E., Jahnke, M. C. & Pape, T. Synthesis of pincer-type bis(benzimidazolin-2-ylidene) palladium complexes and their application in C-C coupling reactions. *Organometallics* **26**, 150–154 (2007).

46. Arnold, P. L. & Casely, I. J. F-block N-heterocyclic carbene complexes. *Chem. Rev.* **109**, 3599–3611 (2009).

47. Hahn, F. E. & Jahnke, M. C. Heterocyclic carbenes: Synthesis and coordination chemistry. *Angew. Chem., Int. Ed.* **47**, 3122–3172 (2008).

48. Liu, X. L. & Chen, W. Z. Pyridazine-based N-heterocyclic carbene complexes and Ruthenium-catalyzed oxidation reaction of alkenes. *Organometallics* **31**, 6614–6622 (2013).

49. Li, Q., Li, X., Yang, J., Song, H. B. & Tang, L. F. Synthesis and structural characterization of N-heterocyclic carbene silver complexes derived from N-ferrocenylmethyl-N′-(pyridylmethyl)imidazolium iodides. *Polyhedron* **59**, 29–37 (2013).

50. Chen, J. H., Zhang, X. Q., Feng, Q. & Luo, M. M. Novel hexadentate imidazolium salts in the rhodium-catalyzed addition of arylboronic acids to aldehydes. *J. Organomet. Chem.* **691**, 470–474 (2006).

51. Sun, Z. X. & Cheng, Y. N-Heterocyclic carbene-catalyzed cascade annulation reaction of o-vinylarylaldehydes with nitrosoarenes: One-step assembly of functionalized 2,3-benzoxazin-4-ones. *Org. Biomol. Chem.* **10**, 4088–4094 (2012).

52. Liu, B., Xia, Q. & Chen, W. Z. Direct synthesis of iron, cobalt, nickel, and copper complexes of N-heterocyclic carbenes by using commercially available metal powders. *Angew. Chem., Int. Ed.* **48**, 5513–5516 (2009).

53. Zhang, F. *et al.* Synthesis of a novel fluorescent anthryl calix[4]arene as picric acid sensor. *Tetrahedron* **69**, 9886–9889 (2013).

54. Papadopoulou, A., Green, R. J. & Frazier, R. A. Interaction of flavonoids with bovine serum albumin: A fluorescence quenching study. *J. Agric. Food Chem.* **53**, 158–163 (2005).

55. Caballero, A. *et al.* Highly selective chromogenic and redox or fluorescent sensors of Hg^{2+} in aqueous environment based on 1,4-disubstituted azines. *J. Am. Chem. Soc.* **127**, 15666–15667 (2005).

56. Liu, K. *et al.* Turn on ESPT: Novel salicylaldehyde based sensor for biological important fluoride sensing. *J. Photochem. Photobiol. B* **138**, 75–79 (2014).

57. Wang, J. S., Bodige, S. G., Watson, W. H. & Gutsche, C. D. Complexation of fullerenes with 5,5′-biscalix[5]arene. *J. Org. Chem.* **65**, 8260–8263 (2000).

58. Polster, J. & Lachmann, H. Spectrometric titrations: VCH, Weinheim. 256–259 (1989).

59. Cao, M. J. *et al.* A dansyl-based fluorescent probe for selectively detecting Cu^{2+} and imaging in living cells. *RSC Adv.* **5**, 23666–23670 (2015).

60. Liu, Q. X. *et al.* Two N-heterocyclic carbene silver(I) cyclophanes: Synthesis, structural studies, and recognition for p-phenylenediamine. *Organometallics* **30**, 3732–3739 (2011).

61. Shang, X. F. *et al.* Colorimeric and fluorescence ON-OFF probe for acetate anion based on thiourea derivative: Theory and experiment. *Spectrochimica Acta A* **103**, 276–281 (2013).

62. SMART 5.0 and SAINT 4.0 for Windows NT, Area Detector Control and Integration Software, Bruker Analytical X-Ray Systems, Inc., Madison, WI, USA (1998).

63. Sheldrick, G. M. SADABS, Program for Empirical Absorption Correction of Area Detector Data, Univ. of Göttingen, Germany (1996).

64. Sheldrick, G. M. SHELXTL 5.10 for Windows NT, Structure Determination Software, Brucker Analytical X-Ray Systems, Inc., Madison, WI, USA (1997).

Acknowledgements

Author Contributions

Q.L. and Z.Z. designed the experiments, analyzed the results and wrote the manuscript. Y.L. and R.H. carried out all the experiments and performed the data analysis. All authors reviewed the manuscript.

Additional Information

Supplementary information accompanies this paper at https://doi.org/10.1038/s41598-018-36916-w.

Competing Interests: The authors declare no competing interests.

Publisher's note: Springer Nature remains neutral with regard to jurisdictional claims in published maps and institutional affiliations.